Impact of Correlation on the Capacity of Multiple Access and Broadcast Channels with MIMO-MRC

Raymond H. Y. Louie, *Student Member, IEEE,* Matthew R. McKay, *Member, IEEE,*
and Iain B. Collings, *Senior Member, IEEE*

***Abstract*—This paper investigates the capacity of multiple-access and broadcast channels with MIMO-MRC systems in spatially correlated environments. We present new capacity approximations which are shown to be accurate. The approximations are based on new simple expansions which we derive for the maximum eigenvalue distribution of correlated Wishart matrices. We then proceed to analyze the affects of correlation and show it is beneficial for capacity. Our results are confirmed through comparison with Monte Carlo simulations.**

***Index Terms*—MIMO systems, correlation, capacity analysis, Rayleigh channels, MIMO MRC.**

I. Introduction

MULTIPLE-INPUT multiple-output (MIMO) antenna systems have recently been extended to environments with multiple terminals, each with multiple antennas. Example application scenarios include a single basestation serving multiple terminals (i.e. subscriber units) in a cellular environment, or a relay node serving multiple terminals (i.e. network nodes) in an ad-hoc network. In this paper, we consider scenarios where only one terminal is active at any one time, and transmits/receives along a single eigenmode corresponding to the largest singular value of their channel matrix. This transmission approach is commonly referred to as MIMO maximum ratio combining (MRC). The motivation is that in the low signal to noise ratio (SNR) regime, MIMO-MRC to a single terminal is the capacity achieving access scheme [1, 2].

MIMO-MRC has been studied in the single terminal case in uncorrelated [3, 4] and semi-correlated Rayleigh channels [5] (i.e. channels with transmit or receive correlation, but not both). Recently, double-correlated Rayleigh channels have been considered by deriving the eigenvalue statistics of double-correlated Wishart matrices [6]. In the absence of channel knowledge or its statistics at the transmitter, correlation can be shown to decrease capacity [7–10]. We will show that for MIMO-MRC with multiple terminals and channel knowledge at the transmitter, capacity *increases* with correlation.

For the multiple terminal case, the capacity of MIMO-MRC in an uncorrelated environment was considered in [11], and was shown to scale double logarithmically with the number of terminals. Systems with transmit correlation and a single receive antenna per terminal were analyzed in [12], and capacity was shown to scale logarithmically with the correlation coefficient. These results, however, do not extend easily to the case of MIMO-MRC systems with either semi- or double-correlation. In addition, the capacity expressions given in [11, 12] are inaccurate for practical numbers of terminals (e.g. < 50).

In this paper, we consider MIMO-MRC systems with multiple terminals and spatial correlation at *either* or *both* the transmitter and receiver ends. We present new accurate capacity approximations by deriving new expansions for the cumulative distribution function (c.d.f.) of the maximum eigenvalue of uncorrelated, semi-, and double-correlated Wishart matrices, and using tools from order statistics. Our results apply for both broadcast and multiple-access channels.

We also analyze the effects of correlation on capacity. We first consider a case with semi-correlation and show that our capacity approximation increases with correlation. We then consider a case with a large number of terminals (with a fixed number of antennas) and quantify the benefits of correlation for both the semi- and double-correlated scenarios. Our results demonstrate that capacity scales logarithmically with the maximum eigenvalue of the correlation matrix at either/both the transmitter or/and receiver end. This generalizes the results of [11, 12] to arbitrary correlation models and multiple antennas. Our results are confirmed through comparison with Monte Carlo simulations.

II. System Model and Capacity

We start by describing the broadcast channel, where the broadcast node has N_t antennas and each of the K terminals has N_r antennas. Considering the case where there is spatial correlation at both the transmitter and the receivers, and employing the common Kronecker model (as used in [6, 7]), the channel between the broadcast node and the kth terminal is given by

$$\mathbf{H}_k = \mathbf{R}_k^{\frac{1}{2}} \mathbf{H}_{w,k} \mathbf{S}^{\frac{1}{2}} \sim \mathcal{CN}_{N_r,N_t}\left(\mathbf{0}_{N_r \times N_t}, \mathbf{R}_k \otimes \mathbf{S}\right) \quad (1)$$

Manuscript received January 31, 2007; revised July 23, 2007; accepted December 25, 2007. The associate editor coordinating the review of this paper and approving it for publication was M. Win. This work has been presented in part at the IEEE Int. Conf. on Communications (ICC), Glasgow UK, July 2007.

R. H. Y. Louie is with the Telecommunications Laboratory, School of Electrical and Information Engineering, University of Sydney, NSW 2006, Australia. He is also with the Wireless Technologies Laboratory, ICT Centre, CSIRO, Epping, NSW 1710, Australia (e-mail: rlouie@ee.usyd.edu.au).

M. R. McKay is with the Department of Electronic and Computer Engineering, Hong Kong University of Science and Technology, Clear Water Bay, Kowloon, Hong Kong (e-mail: eemckay@ust.hk).

I. B. Collings is with the Wireless Technologies Laboratory, ICT Centre, CSIRO, Epping, NSW 1710, Australia (e-mail: iain.collings@csiro.au).

Digital Object Identifier 10.1109/TWC.2008.070126.

where $\mathbf{R}_k \in \mathcal{C}^{N_r \times N_r}$ and $\mathbf{S} \in \mathcal{C}^{N_t \times N_t}$ are the receive and transmit correlation matrices, and $\mathbf{H}_{w,k} \sim \mathcal{CN}_{N_r,N_t}(\mathbf{0}_{N_r \times N_t}, \mathbf{I}_{N_r} \otimes \mathbf{I}_{N_t})$. Note that here we have used standard notation from multivariate statistical theory (see eg. [7]), with $\mathcal{CN}_{N_r,N_t}(\mathbf{0}_{N_r \times N_t}, \mathbf{R}_k \otimes \mathbf{S})$ representing a zero-mean N_r x N_t complex Gaussian matrix, with each of the columns having correlation matrix $\mathbf{R}_k$, and each of the rows having correlation $\mathbf{S}$. Note that the transmit correlation is the same for all channels since the Kronecker model assumes that correlation is dominated by local scatterers. The general model in (1) is referred to as the double-correlated channel model. We will also consider semi-correlated channel models where the correlation is at the end with the least number of antennas; meaning that either $\mathbf{S}$ or all $\mathbf{R}_k$'s are identity. For the multiple-access channel, the channel is defined similarly but with the role of the transmitter and receiver reversed.

We define $\lambda_{\max}^{(k)}$ to be the maximum eigenvalue of $\mathbf{H}_k^\dagger \mathbf{H}_k$, and define $\lambda_{\max,K} \triangleq \max(\lambda_{\max}^{(1)}, ..., \lambda_{\max}^{(K)})$. We also define k_{max} to denote the terminal corresponding to $\lambda_{\max,K}$. For the broadcast channel, the broadcast node sends only to terminal k_{max}. For the multiple-access channel, terminal k_{max} is the only one to transmit to the multiple-access node. In both cases, full channel state information (CSI) is assumed to be known at the receiver, but only the eigenvector corresponding to $\lambda_{\max,K}$ is required at the transmitter. Note that only one terminal is active at any one time.

This form of access protocol is suited to any top layer applications that are delay tolerant, such as file sharing. It is also suited to more general top layer applications whenever the environment is such that the transmission channel changes significantly between packets. From a fairness point of view it is important that each terminal is selected to transmit often enough to meet the delay constraints of the application[1].

The received vector is

$$\mathbf{r} = \sqrt{\bar{\gamma}} \mathbf{H}_{k_{\text{max}}} \mathbf{w} x + \mathbf{n} \quad (2)$$

where x is the transmitted symbol satisfying $E\left[|x|^2\right] = 1$, $\mathbf{w}$ is the $N_t \times 1$ transmit weight vector with $E\left[\|\mathbf{w}\|^2\right] = 1$, $\mathbf{n}$ is the additive noise vector $\sim \mathcal{CN}_{N_r,1}(\mathbf{0}_{N_r \times 1}, \mathbf{I}_{N_r})$, and $\bar{\gamma}$ is the transmit SNR. At the receiver, the signal is multiplied by the vector $\mathbf{w}^\dagger \mathbf{H}_{k_{\text{max}}}^\dagger$, according to the MRC principle, to give

$$z = \mathbf{w}^\dagger \mathbf{H}_{k_{\text{max}}}^\dagger \mathbf{r} = \sqrt{\bar{\gamma}} \mathbf{w}^\dagger \mathbf{H}_{k_{\text{max}}}^\dagger \mathbf{H}_{k_{\text{max}}} \mathbf{w} x + \mathbf{w}^\dagger \mathbf{H}_{k_{\text{max}}}^\dagger \mathbf{n} \ . \quad (3)$$

The SNR at the output of the MRC receiver can be expressed as

$$\gamma = \bar{\gamma} \mathbf{w}^\dagger \mathbf{H}_{k_{\text{max}}}^\dagger \mathbf{H}_{k_{\text{max}}} \mathbf{w} \ . \quad (4)$$

The transmit weight vector which maximizes (4), denoted by $\mathbf{w}_{\text{opt}}$, is the eigenvector corresponding to $\lambda_{\max,K}$ [3]. This gives

$$\gamma = \bar{\gamma} \mathbf{w}_{\text{opt}}^\dagger \mathbf{H}_{k_{\text{max}}}^\dagger \mathbf{H}_{k_{\text{max}}} \mathbf{w}_{\text{opt}} = \bar{\gamma} \lambda_{\max,K} \ . \quad (5)$$

[1]For channels which do not vary sufficiently between packets, more sophisticated access protocols such as proportional fair scheduling and opportunistic beamforming [13] may be needed to guarantee fair channel access amongst the different terminals. The analysis of such algorithms is beyond the scope of this paper

The resulting capacity for the MIMO-MRC system with multiple terminals is given by

$$C_{\text{multi}} = \mathrm{E}[\log_2(1 + \bar{\gamma} \lambda_{\max,K})] \quad (6)$$
$$= \int_0^\infty \log_2(1 + \bar{\gamma} x) f_{\lambda_{\max,K}}(x) \mathrm{d}x \quad (7)$$

where $f_{\lambda_{\max,K}}(\cdot)$ is the probability density function (p.d.f.) of $\lambda_{\max,K}$. Using a result from order statistics [14], (7) can be written as

$$C_{\text{multi}} = \int_0^\infty \log_2(1 + \bar{\gamma} x) \prod_{k=1}^{K} F_{\lambda_{\max}^{(k)}}(x) \left(\sum_{k=1}^{K} \frac{f_{\lambda_{\max}^{(k)}}(x)}{F_{\lambda_{\max}^{(k)}}(x)} \right) \mathrm{d}x \quad (8)$$

where $F_{\lambda_{\max}^{(k)}}(\cdot)$ and $f_{\lambda_{\max}^{(k)}}(\cdot)$ are the c.d.f. and p.d.f. respectively of $\lambda_{\max}^{(k)}$.

This expression can be simplified in situations where the correlation matrices for all terminals are the same (ie. $\mathbf{R}_k = \mathbf{R}$ for the broadcast channel and $\mathbf{S}_k = \mathbf{S}$ for the multiple-access channel for all $k \in \{1, .., K\}$). Practical examples include semi-correlated scenarios with correlation at the broadcast/multiple-access node only, and uncorrelated scenarios. For such scenarios we have

$$C_{\text{multi}} = K \int_0^\infty \log_2(1 + \bar{\gamma} x) f_{\lambda_{\max}}(x) F_{\lambda_{\max}}^{K-1}(x) \mathrm{d}x \quad (9)$$

where $\lambda_{\max}$ is the maximum eigenvalue for an *arbitrary* terminal, with p.d.f. $f_{\lambda_{\max}}(\cdot)$ and c.d.f. $F_{\lambda_{\max}}(\cdot)$.

In general, the integrals in (8) and (9) are hard to solve explicitly, even for the simplest case of a single terminal system ($K = 1$) with uncorrelated Rayleigh fading [15]. In this paper we approximate (9) by

$$C_{\text{multi}} \approx \log_2(1 + \bar{\gamma}\, g(K)) \quad (10)$$

where

$$g(K) = F_{\lambda_{\max}}^{-1} \left(\frac{1}{1 + e^{-\sum_{i=1}^{K-1} \frac{1}{i}}} \right) \ . \quad (11)$$

This expression is obtained by first noting that for a random variable X following a symmetric distribution, with c.d.f. $F_X(\cdot)$ and largest order statistic X_K, we have the following inequality [16]

$$\mathrm{E}[X_K] \leq F_X^{-1} \left(\frac{1}{1 + e^{-\sum_{i=1}^{K-1} \frac{1}{i}}} \right) \ . \quad (12)$$

This upper bound has been shown to be tight for a Gaussian distribution [14]. Now defining $m = \max(N_t, N_r)$ and $n = \min(N_t, N_r)$, $C_{\text{multi}} = E[\log_2(1 + \bar{\gamma} \lambda_{\max,K})]$ converges to a Gaussian distribution for fixed n and as $m \to \infty$ [17]. Thus, we substitute $X = \log_2(1+\bar{\gamma}\lambda_{\max})$ into (12), and apply simple algebraic manipulation to obtain (10).

We will focus on evaluating (10), and show that it yields an accurate approximation for (9). As such, unless otherwise specified, for the remainder of our mathematical analysis we will drop the subscript k from $\mathbf{R}_k$ and $\mathbf{S}_k$. Following this, we will also show that (10) can be used to provide an accurate approximation to (8) in the general cases when the $\mathbf{R}_k$'s (or $\mathbf{S}_k$'s in the multiple-access case) are not all the same, by setting $\mathbf{R}$ (or $\mathbf{S}$) to be the average of the $\mathbf{R}_k$'s (or $\mathbf{S}_k$'s).

TABLE I
$\frac{1}{1+e^{-\sum_{i=1}^{K-1}\frac{1}{i}}}$ FOR DIFFERENT NUMBER OF USERS, K

K	$\frac{1}{1+e^{-\sum_{i=1}^{K-1}\frac{1}{i}}}$
1	0.5
2	0.7311
5	0.8893
10	0.9442
20	0.9720
30	0.9813
50	0.9888
100	0.9944

To calculate (10), we require the inverse function of $F_{\lambda_{\max}}(\cdot)$. Unfortunately, for uncorrelated, semi- and double-correlated scenarios, $F_{\lambda_{\max}}(\cdot)$ is a complicated determinantal function [3,4,6,18], and the inverse calculation is intractable in general. Progress can be made, however, by noting that the argument of the inverse c.d.f. in (10) is close to unity for typical values of K, as shown in Table I. In other words, we are dealing with the tail of the c.d.f.. This result motivates us to derive new expansions for $F_{\lambda_{\max}}(\cdot)$ which are accurate in the tail, and admit simple formulation of the required inverse.

We first define the matrices $\mathbf{\Sigma} \in \mathcal{C}^{m\times m}$ and $\mathbf{\Omega} \in \mathcal{C}^{n\times n}$ with eigenvalues $\sigma_1 < ... < \sigma_m$ and $\omega_1 < ... < \omega_n$ respectively, as follows

$$\mathbf{\Sigma} = \begin{cases} \mathbf{R} & \text{for } N_r > N_t \\ \mathbf{S} & \text{for } N_r \leq N_t \end{cases} \qquad \mathbf{\Omega} = \begin{cases} \mathbf{R} & \text{for } N_r \leq N_t \\ \mathbf{S} & \text{for } N_r > N_t \end{cases} . \tag{13}$$

With these definitions, note that the maximum channel eigenvalue $\lambda_{\max}$ is statistically equivalent to the maximum eigenvalue of a complex Wishart matrix $\mathbf{X}^\dagger\mathbf{X}$, where $\mathbf{X}$ has the following distribution:

- Uncorrelated fading: $\mathbf{X} \sim \mathcal{CN}_{m,n}(\mathbf{0}_{m\times n}, \mathbf{I}_m \otimes \mathbf{I}_n)$
- Semi-correlated fading: $\mathbf{X} \sim \mathcal{CN}_{m,n}(\mathbf{0}_{m\times n}, \mathbf{I}_m \otimes \mathbf{\Omega})$
- Double-correlated fading: $\mathbf{X} \sim \mathcal{CN}_{m,n}(\mathbf{0}_{m\times n}, \mathbf{\Sigma} \otimes \mathbf{\Omega})$

In the following section we will derive new asymptotic expansions for the distribution of $\lambda_{\max}$ for each of these scenarios. We note that although the uncorrelated and semi-correlated scenarios can be seen as special cases of the double-correlated scenario, the results do not decompose easily and will be treated separately. These expressions will then be used to investigate capacity, and to show that correlation increases capacity in multiple terminal MIMO-MRC systems.

As an aside, it is interesting to note that the capacity increase with correlation result indicates that the maximum singular value of $\mathbf{R}^{\frac{1}{2}}\mathbf{H}_w\mathbf{S}^{\frac{1}{2}}$ must be greater than the maximum singular value of $\mathbf{H}_w$ on average; since in uncorrelated channels MIMO-MRC transmits along the maximum singular value of $\mathbf{H}_w$, whereas for the correlated scenarios transmission is along the maximum singular value of $\mathbf{R}^{\frac{1}{2}}\mathbf{H}_w\mathbf{S}^{\frac{1}{2}}$.

III. C.D.F. Expansions for the Maximum Eigenvalue of Complex Wishart Matrices

The following theorem applies to the uncorrelated scenario.

Theorem 1: Let $\mathbf{X} \sim \mathcal{CN}_{m,n}(\mathbf{0}_{m\times n}, \mathbf{I}_m \otimes \mathbf{I}_n)$. The c.d.f. of the maximum eigenvalue of the complex Wishart matrix $\mathbf{X}^\dagger\mathbf{X}$ is given by[2]

$$F_{\lambda_{\max}}(x) = 1 - \alpha_{\text{iid}} e^{-x} \sum_{p=1}^{n}\sum_{q=1}^{n} C_{p,q}K_{p,q} \sum_{t=0}^{\tau+p+q-2} \frac{x^t}{t!} + \mathcal{O}(e^{-2x}x^{2m+2n-4}) \tag{14}$$

where $\alpha_{\text{iid}} = 1/(\prod_{k=1}^{n}(m-k)!(n-k)!)$, $\tau = m-n$, and $C_{p,q}$ is the $(p,q)^{\text{th}}$ cofactor of the $n\times n$ matrix $\mathbf{K}$ with $(i,j)^{\text{th}}$ element $K_{i,j} = \Gamma(\tau+i+j-1)$.

An alternate expansion with slower decaying $\mathcal{O}(\cdot)$ terms is

$$F_{\lambda_{\max}}(x) = 1 - \frac{e^{-x}x^{m+n-2}}{(m-1)!(n-1)!} + \mathcal{O}(e^{-x}x^{m+n-3}) . \tag{15}$$

Proof: The proof follows a similar line of reasoning to the semi-correlated case which we presented in a recent conference paper [19], and is omitted due to space constraints. ■

Note that (15) can also be obtained by integrating the p.d.f. derived in [11].

The following theorem applies to the semi-correlated scenario.

Theorem 2: Let $\mathbf{X} \sim \mathcal{CN}_{m,n}(\mathbf{0}_{m\times n}, \mathbf{I}_m \otimes \mathbf{\Omega})$. Then the c.d.f. of the maximum eigenvalue of the complex Wishart matrix $\mathbf{X}^\dagger\mathbf{X}$ is given by

$$F_{\lambda_{\max}}(x) = 1 - \alpha_{\text{semi}} e^{-\frac{x}{\omega_n}} \sum_{p=1}^{n} D_{p,n}V_{p,n} \sum_{t=0}^{m-p} \frac{\left(\frac{x}{\omega_n}\right)^t}{t!} + \mathcal{O}(e^{-\frac{x}{\omega_{n-1}}}x^{m-1}) \tag{16}$$

where $\alpha_{\text{semi}} = 1/\det(\mathbf{V})$, and $D_{p,n}$ is the $(p,n)^{\text{th}}$ cofactor of the $n\times n$ matrix $\mathbf{V}$ with $(i,j)^{\text{th}}$ element $V_{i,j} = 1/\omega_j^{i-1}$ and $\omega_1 < ... < \omega_n$ are the eigenvalues of $\mathbf{\Omega}$.

An alternate expansion with slower decaying $\mathcal{O}(\cdot)$ terms is

$$F_{\lambda_{\max}}(x) = 1 - \frac{\omega_n^{n-m}x^{m-1}e^{-\frac{x}{\omega_n}}}{(m-1)!\prod_{i=1}^{n-1}(\omega_n-\omega_i)} + \mathcal{O}(e^{-\frac{x}{\omega_n}}x^{m-2}) . \tag{17}$$

Proof: See [19]. ■

The following theorem applies to the double-correlated scenario.

Theorem 3: Let $\mathbf{X} \sim \mathcal{CN}_{m,n}(\mathbf{0}_{m\times n}, \mathbf{\Sigma} \otimes \mathbf{\Omega})$. Then the c.d.f. of the maximum eigenvalue of the complex Wishart matrix $\mathbf{X}^\dagger\mathbf{X}$ is given by

$$F_{\lambda_{\max}}(x) = 1 - \frac{e^{-\frac{x}{\omega_n\sigma_m}}\omega_n^{n-1}\sigma_m^{m-1}}{\prod_{i=1}^{m-1}(\sigma_m-\sigma_i)\prod_{i=1}^{n-1}(\omega_n-\omega_i)} + \mathcal{O}(e^{-\frac{x}{\varphi}}x^{-1}) \tag{18}$$

where $\varphi = \omega_n\sigma_{m-1}$ for $\sigma_m < \omega_n$, and $\varphi = \omega_{n-1}\sigma_m$ for $\sigma_m >= \omega_n$. Also, $\sigma_1 < ... < \sigma_m$ are the eigenvalues of $\mathbf{\Sigma}$ and $\omega_1 < ... < \omega_n$ are the eigenvalues of $\mathbf{\Omega}$.

Proof: See Appendix A. ■

Since we are interested in the tail of the c.d.f., we define $\hat{F}_{\lambda_{\max}}(x)$ to be $F_{\lambda_{\max}}(x)$ given in the theorems above, but without the $\mathcal{O}(\cdot)$ term. Note that in all three cases, $\hat{F}_{\lambda_{\max}}(x)$

[2] $f(x) = \mathcal{O}(g(x))$ means there exists a non-negative constant α such that $\lim_{x\to\infty} |\frac{f(x)}{g(x)}| \leq \alpha$.

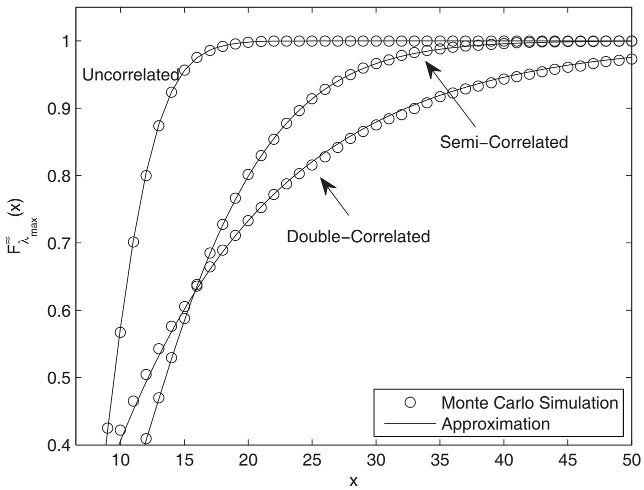

Fig. 1. C.d.f. of the maximum eigenvalue of complex Wishart matrices, for different correlation scenarios. The curves are for $N_t = 4$ and $N_r = 4$, with correlation parameters: $\sigma_t^2 = \sigma_r^2 = \pi/30$, $\theta_t = \theta_r = \frac{\pi}{2}$ and $d_t = d_r = \frac{1}{2}$.

is of the form $1 - e^{-ax}J(x)$, where a is a non-negative real number and $J(x)$ is a polynomial.

Fig. 1 shows $\hat{F}_{\lambda_{\max}}(x)$ for the uncorrelated (14), semi- (16), and double-correlated (18) scenarios. The correlation matrices were constructed using the practical channel model from [20] with its associated correlation parameters θ_t, θ_r, σ_r^2, σ_t^2, d_t and d_r. Clearly our new simple expansions are accurate in each case.

IV. Capacity Approximations

This section presents new approximations to the capacity for the three correlation scenarios under consideration.

A. Uncorrelated and Semi-Correlated Scenarios

Capacity approximations for the uncorrelated and semi-correlated scenarios are obtained by substituting $\hat{F}_{\lambda_{\max}}(x)$ based on (14) and (16) respectively, into (10). We evaluate $\hat{g}(K) = \hat{F}_{\lambda_{\max}}^{-1}\left(\frac{1}{1+e^{-\sum_{i=1}^{K-1}\frac{1}{i}}}\right)$ by starting with $\hat{g}_0(K) = 1$, and iterating the following expression

$$\hat{g}_{j+1}(K) = \frac{1}{a}\left(\ln\left(J(\hat{g}_j(K))\right) + \ln(N(K))\right) \qquad (19)$$

until convergence where $N(K) = 1 + e^{\sum_{i=1}^{K-1}\frac{1}{i}}$, and where for the uncorrelated case

$$\begin{cases} a = 1 \\ J(x) = \alpha_{\text{iid}} \sum_{p=1}^{n} \sum_{q=1}^{n} C_{p,q} K_{p,q} \sum_{t=0}^{\tau+p+q-2} \frac{x^t}{t!} \end{cases} \qquad (20)$$

and for the semi-correlated case

$$\begin{cases} a = \frac{1}{\omega_n} \\ J(x) = \alpha_{\text{semi}} \sum_{p=1}^{n} D_{p,n} V_{p,n} \sum_{t=0}^{m-p} \frac{(ax)^t}{t!} \end{cases} . \qquad (21)$$

Simulations indicate that (19) has a fast rate of convergence. The exact rate, however, depends on the number of antennas and correlation in the system. For example, using the same semi-correlated scenario and antenna configuration in Fig. 1, running the iteration only 5 times for $F_{\lambda_{\max}}(x) = 0.833$ results in an almost negligible error of only 0.06%.

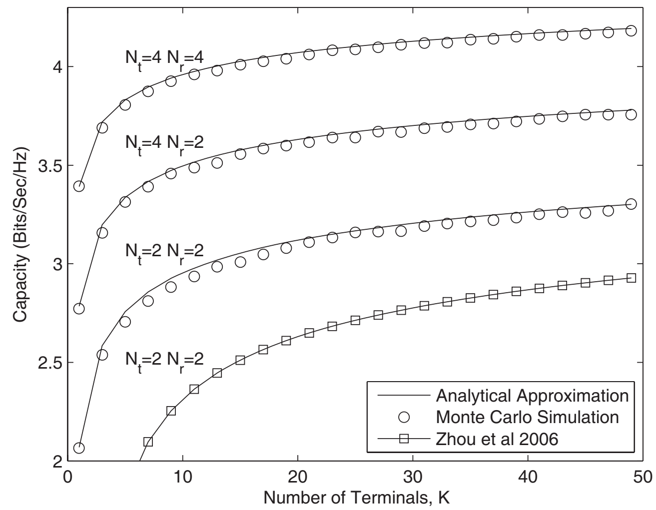

Fig. 2. Capacity of multiuser MIMO-MRC in uncorrelated Rayleigh fading, with SNR $\bar{\gamma} = 0$ dB.

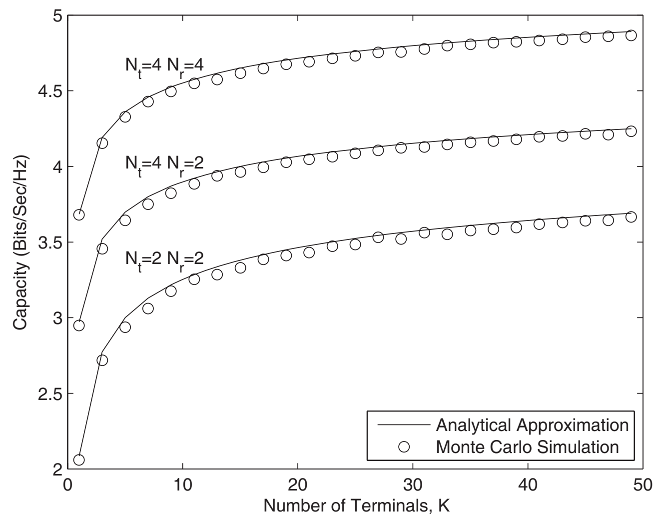

Fig. 3. Capacity of multiuser MIMO-MRC in semi- (receive) correlated Rayleigh fading, with SNR $\bar{\gamma} = 0$ dB, and correlation parameters: $\sigma_r^2 = \pi/15$, $\theta_r = \frac{\pi}{2}$, $d_r = \frac{1}{2}$.

We denote $g_{\text{conv}}(K)$ to be the converged value from (19). Substituting this into (10) in place of $g(K)$ gives an approximation to capacity as follows

$$C_{\text{multi}} \approx \log_2(1 + \bar{\gamma} g_{\text{conv}}(K)) . \qquad (22)$$

Fig. 2 shows the capacity for uncorrelated fading, for different N_t and N_r. The analytical approximation curves were obtained using (19), (20) and (22). We see that these curves accurately approximate the Monte Carlo simulated curves in all cases. For comparison, we also present the previous capacity approximation from [11], for the case of 2×2 antennas. We clearly see that our new approximation is much more accurate for all practical K values.

Fig. 3 shows the capacity for semi-correlated fading (receive correlation), for different N_t and N_r. The analytical approximation curves were obtained using (19), (21) and (22). Again, we see that the analytical curves accurately approximate the Monte Carlo simulated curves in all cases.

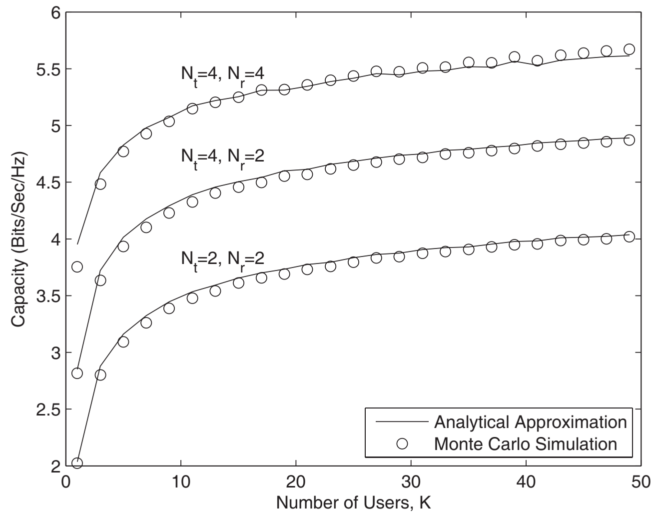

Fig. 4. Capacity of multiuser MIMO-MRC in double-correlated Rayleigh fading, with SNR $\bar{\gamma} = 0$ dB, and correlation parameters: $\sigma_t^2 = \pi/30$, $\theta_t = \theta_r = \frac{\pi}{2}$, $d_t = d_r = \frac{1}{2}$. The receive angular spread σ_r^2 is randomly generated from a uniform distribution with values ranging from 0 to $\frac{\pi}{4}$.

B. Double-Correlated Scenario

For the double-correlated case, we obtain capacity approximations by taking the average of the correlation matrices of each terminal. More formally, denoting the correlation matrix of the kth terminal by $\mathbf{\Omega}_k$[3], and defining the *average* correlation matrix $\bar{\mathbf{\Omega}} = \frac{1}{K}\sum_{k=1}^{K} \mathbf{\Omega}_k$ with eigenvalues $\bar{\omega}_1 < ... < \bar{\omega}_n$, we start by substituting $\hat{F}_{\lambda_{\max}}(x)$ in (18) into (10), but replacing $\mathbf{\Omega}$ by $\bar{\mathbf{\Omega}}$. We then proceed along similar lines as for the uncorrelated and semi-correlated cases and substitute

$$\begin{cases} a = \frac{1}{\bar{\omega}_n \sigma_m} \\ J(x) = J = \frac{\bar{\omega}_n^{n-1}\sigma_m^{m-1}}{\prod_{i=1}^{m-1}(\sigma_m - \sigma_i)\prod_{i=1}^{n-1}(\bar{\omega}_n - \bar{\omega}_i)} \end{cases} \tag{23}$$

into the iterative algorithm (19), and substitute the converged value $g_{\text{conv}}(K)$ into (22) to obtain the desired capacity approximation.

Fig. 4 shows the capacity for the double-correlated case, for different N_t and N_r, considering a scenario where there is high correlation at the transmitter, and different correlation at the receivers. The receive correlation matrices were randomly generated by varying the receive angular spread σ_r^2 according to an uniform distribution ranging from 0 to $\frac{\pi}{4}$. The capacity approximations were generated using (22). We see that our analytical approximation curves accurately approximate the Monte Carlo simulated curves in all cases.

V. Effect of Correlation on Capacity

This section explores the intuitive notion that the beamforming approach of MIMO-MRC can successfully exploit the spatial selectivity arising in channels exhibiting spatial correlation, in the case of systems with multiple communicating terminals. In other words we are interested in finding out whether correlation increases capacity for MIMO-MRC systems with multiple terminals. While we conjecture that this is always true for all system parameter values, it is difficult to prove, and harder to quantify. In the following sections we consider three special cases.

A. Semi-Correlated $2 \times m$

In this first case we consider a $2 \times m$ system with semi-correlation. For this system we are able to derive an analytical condition under which the capacity approximation derived in Section IV increases with correlation; given in the following lemma. Note that while this is not a necessary condition, it is sufficient.

Lemma 1: The capacity approximation given in (10) for the semi-correlated $2 \times m$ case increases with correlation if

$$\frac{1}{1 + e^{-\sum_{i=1}^{K-1} \frac{1}{i}}} \geq F_{\lambda_{\max}}\left(m\omega_1 + \frac{{\omega_1}^2 + {\omega_2}^2}{\omega_2 - \omega_1}; \omega_1, \omega_2\right) \tag{24}$$

where $F_{\lambda_{\max}}(\cdot;\cdot,\cdot)$ is given in (52).

Proof: See Appendix B. ■

The condition in Lemma 1 can be easily calculated numerically using (52).

Fig. 5 plots curves showing the case of equality in (24). The equality determines the minimum (or threshold) value of ω_2 (the maximum eigenvalue of the correlation matrix $\mathbf{\Omega}$) for which (24) is satisfied. The corresponding values of ω_1 are obtained by substituting $\omega_1 = 2-\omega_2$. The curves are shown as a function of the number of receive antennas, m, for different numbers of terminals, K. For example, when $m = 6$ and $K = 5$, (24) is satisfied when $1.15 \leq \omega_2 \leq 2$. From the figure we can see that the ω_2 threshold values are much closer to 1 than they are to 2, so clearly the condition in Lemma 1 holds for most correlation scenarios.

Fig. 6 shows curves for capacity vs. ω_2, obtained via Monte Carlo simulations, for $m = 5$, and for different K. Also shown are the threshold values of ω_2 derived from (24), as described above for Fig. 5, indicated here by circles. The figure shows that, as conjectured, capacity is an increasing function of correlation for all values of correlation, even below the values predicted in (24).

B. Double-Correlated Numerical Analysis

In this second case we consider double-correlation and show that again, correlation increases capacity. Fig. 7 shows the capacity for a 5×2 system with different numbers of users, K. The horizontal axis corresponds to antenna correlation in the following way. The correlation matrix for each terminal is different, and is generated by randomly selecting an angular spread according to an uniform distribution from 0 to a particular upper limit. The horizontal axis of the graph shows the upper limit for each scenario. Fig. 7 clearly shows that capacity increases with increasing correlation at the receiving terminals. Again, we see that our analytical approximations are an accurate approximation to the Monte Carlo simulated curves.

[3]Note that here we assume that the broadcast/multiple-access node has the most antennas. Derivation of capacity approximations for the case where the broadcast/multiple-access node has the least antennas is straightforward.

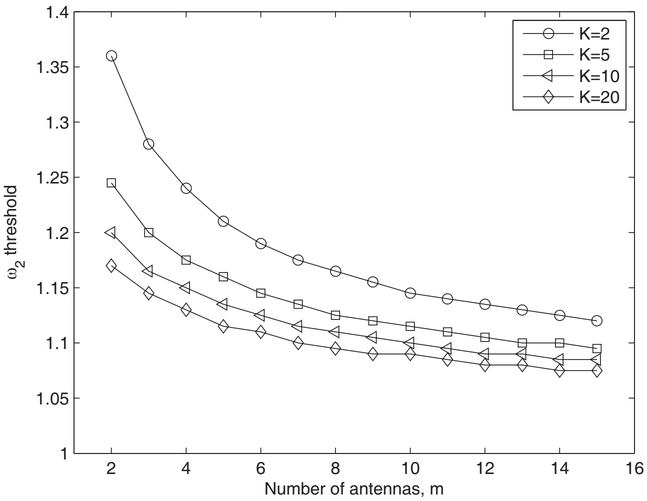

Fig. 5. Minimum (or threshold) value of the maximum eigenvalue ω_2 of the correlation matrix $\mathbf{\Omega}$, for which the condition (24) is satisfied.

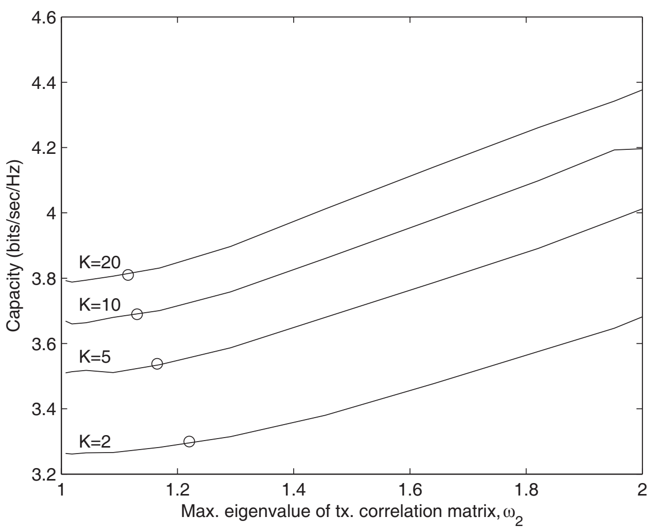

Fig. 6. Capacity of multiuser MIMO-MRC in semi-correlated Rayleigh fading vs the maximum eigenvalue ω_2 of the correlation matrix $\mathbf{\Omega}$ with SNR $\bar{\gamma} = 0$ dB, and correlation parameters: $\theta_t = \frac{\pi}{2}$, $d_t = \frac{1}{2}$. The ω_2 values are generated by varying the transmit angular spread σ_t^2. Circles indicate the minimum value of ω_2 such that the condition (24) holds.

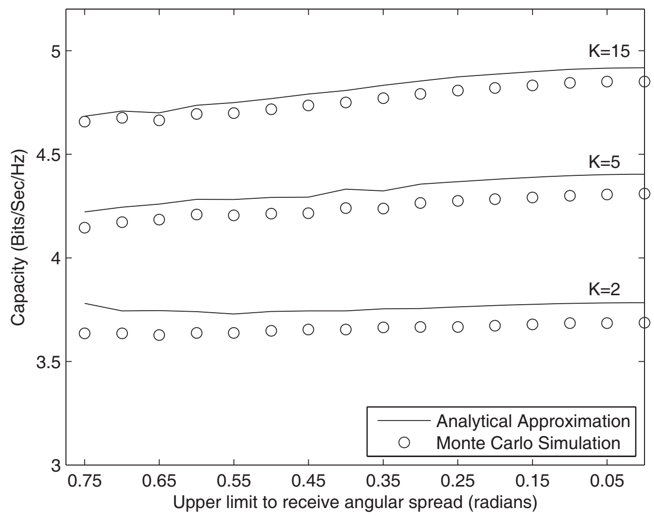

Fig. 7. Capacity of multiuser MIMO-MRC in double-correlated Rayleigh fading with SNR $\bar{\gamma} = 0$ dB, $N_t = 5$, $N_r = 2$ and correlation parameters: $\theta_r = \theta_t = \frac{\pi}{2}$, $d_r = d_t = \frac{1}{2}$ and $\sigma_t^2 = \pi/30$. The correlation matrices for each user are randomly generated by selecting their receive angular spread σ_r^2 from an uniform distribution ranging from 0 to 'upper limit'.

C. Large Number of Users, K

In this third case we examine the capacity behavior in the *large-K* regime for the uncorrelated, semi- and double-correlated scenarios.

The following theorem shows that there is a 'capacity offset' due to correlation in the semi- and double-correlated scenarios. The capacity offset is defined as the constant offset in capacity taken with respect to the reference uncorrelated channel, as $K \to \infty$. Note that in the double-correlated scenario, the theorem is limited to the case when all terminals have the same correlation. (As demonstrated previously, when the terminals have different correlation matrices the capacity can be approximated accurately by assuming that the terminals all have the same correlation, given by the average of their original correlation matrices.)

Theorem 4: For sufficiently large K,

$$\begin{aligned} C_{\mathrm{multi}} &= \log_2 \ln K + \log_2 \bar{\gamma} + \mathrm{CO}_\infty \\ &\quad + \log_2 \left(1 + \mathcal{O}\left(\frac{\ln \ln K}{\ln K}\right)\right) \end{aligned} \tag{25}$$

where CO_∞ is the *capacity offset*, given for the uncorrelated, semi- and double-correlated scenarios as follows

$$\mathrm{CO}_\infty = \begin{cases} 0 & \text{uncorrelated} \\ \log_2(\omega_n) & \text{semi-correlated} \\ \log_2(\omega_n \sigma_m) & \text{double-correlated} \end{cases} \tag{26}$$

Proof: See Appendix C. ■

Note that in the uncorrelated case, a different expression for the asymptotic capacity was given previously in [11].

Clearly, for $\mathbf{\Omega} \neq \mathbf{I}_n$ and $\mathbf{\Sigma} \neq \mathbf{I}_m$, we have $\omega_n > 1$ and $\sigma_m > 1$ respectively, and as such (26) indicates that the capacity increases with correlation. This shows that correlation at the transmitter and/or receiver is beneficial for capacity.

Note that CO_∞ can be viewed as either the reduction in terminals required to achieve a certain capacity for a given $\bar{\gamma}$, or the reduction in $\bar{\gamma}$ needed to achieve a certain capacity for a large number of terminals. Note also that CO_∞ is a similar concept to the high-SNR power offset considered in [21].

Fig. 8 shows capacity curves for the uncorrelated and double-correlated case obtained by using the analytical approximations given in (20), (23) and (22), and compares them with the large terminal capacity expression obtained in (25). The capacity offset is clearly observed.

VI. Conclusion

We have derived accurate approximations for the capacity of multiple-access and broadcast channels in MIMO-MRC systems with correlation. Our results indicate that correlation increases the capacity, compared with uncorrelated scenarios. We have explicitly shown this in a semi-correlated $2 \times m$ case and in the semi- and double-correlated case for a large number of terminals with an arbitrary number of antennas.

$$F_{\lambda_{\max}}(x) = \frac{(-1)^n \Gamma_n(n) \det(\mathbf{\Omega})^{n-1} \det(\mathbf{\Sigma})^{m-1} \det(\mathbf{\Psi}(x))}{\Delta_n(\mathbf{\Omega}) \Delta_m(\mathbf{\Sigma}) (-x)^{n(n-1)/2}}, \tag{27}$$

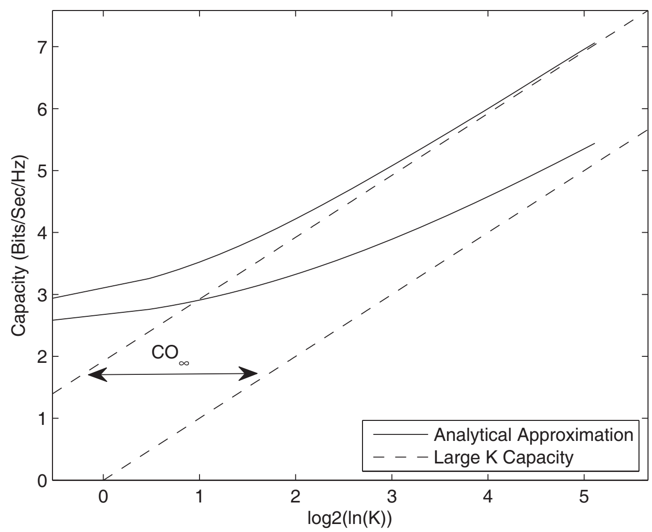

Fig. 8. Capacity vs $\log_2 \ln K$ in uncorrelated and double-correlated scenario, with SNR $\bar{\gamma} = 0$ dB and correlation parameters: $\sigma_r^2 = \sigma_t^2 = \pi/30$, $\theta_t = \theta_r = \frac{\pi}{2}$, $d_t = d_r = \frac{1}{2}$.

Appendix

A. Proof of Theorem 3

The exact c.d.f. is given by [6, Theorem 1] (see (27)) where $\Gamma_n(m) = \prod_{i=1}^{n} \Gamma(m-i+1)$ and $\Delta_m(\cdot)$ is a Vandermonde determinant in the eigenvalues of the $m \times m$ matrix argument, given by [4]

$$\Delta_m(\mathbf{\Sigma}) = \det(\sigma_i^{j-1}) = \prod_{i<j}^{m} (\sigma_j - \sigma_i). \tag{28}$$

Also, $\mathbf{\Psi}(x)$ is a $m \times m$ matrix with $(i,j)^{th}$ element

$$\mathbf{\Psi}(x)_{i,j} = \begin{cases} \left(\frac{1}{\sigma_j}\right)^{m-i} & \text{for } i \leqslant \tau \\ e^{-\frac{x}{\omega_{i-\tau}\sigma_j}} P\left(m; -\frac{x}{\omega_{i-\tau}\sigma_j}\right) & \text{for } i > \tau \end{cases} \tag{29}$$

where $\tau = m - n$, and

$$P(l; y) = 1 - e^{-y} \sum_{k=0}^{l-1} \frac{y^k}{k!} \tag{30}$$

is the regularized lower incomplete gamma function.

We seek an asymptotic expansion of (27) for large x. This will be immediate from an asymptotic expansion of $\det(\mathbf{\Psi}(x))$. To this end, we find it convenient to first re-express this determinant, as detailed in the following. Applying the definition (30) in (29), and then performing successive applications of the multi-linear property of determinants to rows $i > \tau$, we find that

$$\det(\mathbf{\Psi}(x)) = \sum_{\ell=0}^{n} (-1)^{n-\ell} \sum_{\{\underline{\beta}_\ell\}} \det\left(\mathbf{\Psi}_{\underline{\beta}_\ell}(x)\right) \tag{31}$$

where the second summation is over the set of all possible $\underline{\beta}_\ell$, where $\underline{\beta}_\ell$ is defined as

$$\underline{\beta}_\ell = \{\beta_1 < \ldots < \beta_\ell\} \subseteq \{\tau+1, \ldots, m\} \tag{32}$$

and $\mathbf{\Psi}_{\underline{\beta}_\ell}(x)$ is a $m \times m$ matrix with $(i,j)^{\text{th}}$ element

$$\mathbf{\Psi}_{\underline{\beta}_\ell}(x)_{i,j} = \begin{cases} \left(\frac{1}{\sigma_j}\right)^{m-i} & \text{for } i \leqslant \tau \\ e^{-\frac{x}{\omega_{i-\tau}\sigma_j}} & \text{for } i \in \underline{\beta}_\ell, i > \tau \\ \sum_{k=0}^{m-1} \frac{\left(-\frac{x}{\omega_{i-\tau}\sigma_j}\right)^k}{k!} & \text{for } i \notin \underline{\beta}_\ell, i > \tau \end{cases} \tag{33}$$

Note that this form is particularly convenient for deriving an asymptotic expansion as x becomes large. Specifically, from (33) and the definition of the determinant, we see that as x grows large, $\det\left(\mathbf{\Psi}_{\underline{\beta}_\ell}(x)\right)$ decays to 0 as the product of ℓ decaying exponentials and $n-\ell$ polynomial terms in x. Hence, for large x, the determinant sum in (42) is dominated by the terms corresponding to $\ell = 0$ and $\ell = 1$. Consider the case $\ell = 0$. Using repeated application of the multi-linear property, we can write

$$\det\left(\mathbf{\Psi}_{\underline{\beta}_0}(x)\right) = \sum_{k_1=0}^{m-1} \cdots \sum_{k_n=0}^{m-1} \det\left(\mathbf{\Psi}_{\underline{\beta}_0,\{k_1,\ldots,k_n\}}(x)\right) \tag{34}$$

$$= \sum_{0 \le k_1 < \ldots < k_n \le m-1} \sum_{\{\underline{\alpha}\}} \det\left(\mathbf{\Psi}_{\underline{\beta}_0,\underline{\alpha}}(x)\right) \tag{35}$$

where $\{\underline{\alpha}\}$ is the set of permutations $\underline{\alpha} = \{\alpha_1, \ldots, \alpha_n\}$ of the numbers $\{k_1, \ldots, k_n\}$, and $\mathbf{\Psi}_{\underline{\beta}_0,\underline{\alpha}}(x)$ is a $m \times m$ matrix with $(i,j)^{\text{th}}$ element

$$\mathbf{\Psi}_{\underline{\beta}_0,\underline{\alpha}}(x)_{i,j} = \begin{cases} \left(\frac{1}{\sigma_j}\right)^{m-i} & \text{for } i \leqslant \tau \\ \frac{\left(-\frac{x}{\omega_{i-\tau}\sigma_j}\right)^{\alpha_{i-\tau}}}{\alpha_{i-\tau}!} & \text{for } i > \tau \end{cases}. \tag{36}$$

Note that (35) followed from (34) by noting that the determinants in (34) are zero whenever any of the k_i's are equal. Removing row factors now yields

$$\det\left(\mathbf{\Psi}_{\underline{\beta}_0}(x)\right) = \sum_{0 \le k_1 < \ldots < k_n \le m-1} (-x)^{\sum_{i=1}^{n} k_i} \left(\prod_{i=1}^{n} \frac{1}{k_i!}\right) \times \sum_{\{\underline{\alpha}\}} \left(\prod_{i=1}^{n} \frac{1}{\omega_i^{\alpha_i}}\right) \det\left(\tilde{\mathbf{\Psi}}_{\underline{\beta}_0,\underline{\alpha}}(x)\right) \tag{37}$$

[4]Here we introduce the compact notation for the determinant of a matrix, written in terms of the $(i,j)^{\text{th}}$ element.

where $\tilde{\mathbf{\Psi}}_{\underline{\beta}_0,\underline{\alpha}}(x)$ is a $m \times m$ matrix with $(i,j)^{\text{th}}$ element

$$\tilde{\mathbf{\Psi}}_{\underline{\beta}_0,\underline{\alpha}}(x)_{i,j} = \begin{cases} \left(\frac{1}{\sigma_j}\right)^{m-i} & \text{for } i \leqslant \tau \\ \left(\frac{1}{\sigma_j}\right)^{\alpha_{i-\tau}} & \text{for } i > \tau \end{cases} . \quad (38)$$

Now the determinant of (38) is zero whenever $\underline{\alpha}$ (or $\{k_1, \ldots, k_n\}$) has any element taking a value from $\{m-\tau, \ldots, m-1\}$. Therefore after some algebraic maniuplation, (37) becomes (39) where $\underline{\alpha}$ is now simply the set of permutations of $\{0, \ldots, n-1\}$. Re-ordering rows and using the definition of the determinant, we have

$$\begin{aligned} \det\left(\mathbf{\Psi}_{\underline{\beta}_0}(x)\right) &= \frac{(-x)^{n(n-1)/2}}{\Gamma_n(n)} \det\left(\tilde{\mathbf{\Psi}}_{\underline{\beta}_0,\{0,\ldots,n-1\}}(x)\right) \\ &\quad \times \sum_{\{\underline{\alpha}\}} (-1)^{\text{per}(\underline{\alpha})} \left(\prod_{i=1}^{n} \frac{1}{\omega_i^{\alpha_i}}\right) \\ &= \frac{(-x)^{n(n-1)/2}}{\Gamma_n(n)} (-1)^{n(n-1)/2} (-1)^{m(m-1)/2} \\ &\quad \times \det\left(\left(\frac{1}{\omega_i}\right)^{j-1}\right) \det\left(\left(\frac{1}{\sigma_i}\right)^{j-1}\right) \end{aligned} \quad (40)$$

where $\text{per}(\underline{\alpha})$ is the inversion number of $\underline{\alpha}$. Next, we use (28) and [6, Eq. (56)] to give

$$\det\left(\mathbf{\Psi}_{\underline{\beta}_0}(x)\right) = \frac{(-x)^{n(n-1)/2}}{\Gamma_n(n)} \frac{\Delta_n(\mathbf{\Omega})\Delta_m(\mathbf{\Sigma})}{\det(\mathbf{\Omega})^{n-1}\det(\mathbf{\Sigma})^{m-1}} . \quad (41)$$

We can now substitute (41) into (31) to re-write the c.d.f. of $\lambda_{\max}$ in (27) as follows

$$\begin{aligned} F_{\lambda_{\max}}(x) &= 1 + \frac{\Gamma_n(n)\det(\mathbf{\Omega})^{n-1}\det(\mathbf{\Sigma})^{m-1}}{\Delta_n(\mathbf{\Omega})\Delta_m(\mathbf{\Sigma})(-x)^{n(n-1)/2}} \\ &\quad \times \sum_{\ell=1}^{n} (-1)^{\ell} \sum_{\{\underline{\beta}_\ell\}} \det\left(\mathbf{\Psi}_{\underline{\beta}_\ell}(x)\right) . \end{aligned} \quad (42)$$

We now consider the expansion when $\ell = 1$ in (42), which gives

$$\begin{aligned} F_{\lambda_{\max}}(x) &= 1 - \frac{\Gamma_n(n)\det(\mathbf{\Omega})^{n-1}\det(\mathbf{\Sigma})^{m-1}}{\Delta_n(\mathbf{\Omega})\Delta_m(\mathbf{\Sigma})(-x)^{n(n-1)/2}} \\ &\quad \times \sum_{\{\underline{\beta}_1\}} \det\left(\mathbf{\Psi}_{\underline{\beta}_1}(x)\right) + \mathcal{O}(e^{-x(\frac{1}{\omega_n\sigma_m}+\frac{1}{\varphi})} x^{\frac{n(2m-1-n)}{2}}) . \end{aligned} \quad (43)$$

We now simplify the determinant sum in (43). Using Laplaces' expansion we can write

$$\begin{aligned} \sum_{\{\underline{\beta}_1\}} \det\left(\mathbf{\Psi}_{\underline{\beta}_1}(x)\right) &= \sum_{t=\tau+1}^{m} \sum_{r=1}^{m} (-1)^{r+t} e^{-\frac{x}{\omega_{t-\tau}\sigma_r}} \\ &\quad \times \det\left(\underline{\mathbf{\Psi}}^{(t,r)}(x)\right) \end{aligned} \quad (44)$$

where $\underline{\mathbf{\Psi}}^{(t,r)}(x)$ corresponds to the $m \times m$ matrix $\underline{\mathbf{\Psi}}(x)$ with elements

$$\underline{\mathbf{\Psi}}(x)_{i,j} = \begin{cases} \left(\frac{1}{\sigma_j}\right)^{m-i} & \text{for } i \leqslant \tau \\ \sum_{k=0}^{m-1} \frac{\left(-\frac{x}{\omega_{i-\tau}\sigma_j}\right)^k}{k!} & \text{for } i > \tau \end{cases} \quad (45)$$

but with the t^{th} row and r^{th} column removed. Proceeding as in (34)–(35), by repeated application of the multi-linear determinant property to rows $i > \tau$ in the determinants in (44), we can write

$$\det\left(\underline{\mathbf{\Psi}}^{(t,r)}(x)\right) = \sum_{0 \le k_1 < \ldots < k_n \le m-1} \sum_{\{\underline{\alpha}\}} \det\left(\mathbf{\Psi}^{(t,r)}_{\underline{\beta}_0,\underline{\alpha}}(x)\right) \quad (46)$$

where $\mathbf{\Psi}_{\underline{\beta}_0,\underline{\alpha}}(x)$ is defined as in (36), and $\{\underline{\alpha}\}$ is now the set of all permutations $\underline{\alpha} = \{\alpha_1, \ldots, \alpha_{t-1}, \alpha_{t+1}, \ldots, \alpha_n\}$ of the numbers $\{k_1, \ldots, k_{t-1}, k_{t+1}, \ldots k_n\}$. Removing row factors yields

$$\begin{aligned} \det\left(\underline{\mathbf{\Psi}}^{(t,r)}(x)\right) &= \sum_{0 \le k_1 < \ldots < k_n \le m-1} (-x)^{\sum_{i=1, i \neq t-\tau}^{n} k_i} \\ &\times \left(\prod_{i=1, i \neq t-\tau}^{n} \frac{1}{k_i!}\right) \sum_{\{\underline{\alpha}\}} \left(\prod_{i=1, i \neq t-\tau}^{n} \frac{1}{\omega_i^{\alpha_i}}\right) \det\left(\tilde{\mathbf{\Psi}}^{(t,r)}_{\underline{\beta}_0,\underline{\alpha}}(x)\right) \end{aligned} \quad (47)$$

where $\tilde{\mathbf{\Psi}}_{\underline{\beta}_0,\underline{\alpha}}(x)$ is defined as in (38). For large x, the summation in (47) is dominated by terms with the largest exponent of x (i.e. the sets of k_i's which yield the largest sum). In addition, recall that in order for the determinants on the right-hand side of (38) to be non-zero, we require that $k_i < n$ for all i, and that these k_is be unequal. Hence, at large x we can write

$$\begin{aligned} \det\left(\mathbf{\Psi}^{(t,r)}(x)\right) &= (-x)^{\sum_{i=2}^{n}(i-1)} \left(\prod_{i=2}^{n} \frac{1}{(i-1)!}\right) \\ &\times \sum_{\{\underline{\alpha}\}} \left(\prod_{i=1, i \neq t-\tau}^{n} \frac{1}{\omega_i^{\alpha_i}}\right) \det\left(\tilde{\mathbf{\Psi}}^{(t,r)}_{\underline{\beta}_0,\underline{\alpha}}(x)\right) + \mathcal{O}(x^{\frac{n(n-1)}{2}-1}) \\ &= \frac{(-x)^{n(n-1)/2}}{\Gamma_n(n)} \sum_{\{\underline{\alpha}\}} \left(\prod_{i=1, i \neq t-\tau}^{n} \frac{1}{\omega_i^{\alpha_i}}\right) \det\left(\tilde{\mathbf{\Psi}}^{(t,r)}_{\underline{\beta}_0,\underline{\alpha}}(x)\right) \\ &\quad + \mathcal{O}(x^{\frac{n(n-1)}{2}-1}) \end{aligned} \quad (48)$$

where $\underline{\alpha}$ is now simply the set of permutations of $\{1, \ldots, n-1\}$. Now performing manipulations along the lines of (40)-(41) we obtain

$$\begin{aligned} \det\left(\mathbf{\Psi}^{(r,t)}(x)\right) &= \frac{(-x)^{n(n-1)/2}}{\Gamma_n(n)} \frac{\Delta_n^{(t-\tau)}(\mathbf{\Omega})\Delta_m^{(r)}(\mathbf{\Sigma})}{\det(\mathbf{\Omega})^{n-1}\det(\mathbf{\Sigma})^{m-1}} \\ &\quad \times \sigma_r^{m-1}\omega_t^{n-1} + \mathcal{O}(x^{\frac{n(n-1)}{2}-1}) \end{aligned} \quad (49)$$

where $\Delta_n^{(t)}(\mathbf{\Omega})$ and $\Delta_m^{(r)}(\mathbf{\Sigma})$ are Vandermonde determinants in $\{\omega_1, \ldots, \omega_{t-1}, \omega_{t+1}, \ldots, \omega_n\}$ and $\{\sigma_1, \ldots, \sigma_{r-1}, \sigma_{r+1}, \ldots, \sigma_m\}$ respectively. Finally, we substitute (49) into (44) and (43), and consider only the largest exponent of the exponential to obtain the desired result in (18).

B. *Proof of Lemma 1*

For this proof, we invoke the following results from majorization theory[5]. Consider two vectors $\mathbf{x}, \mathbf{y} \in \Re^q$. We

[5] Other related papers have also used results from majorization theory [22, 23].

$$\det\left(\boldsymbol{\Psi}_{\underline{\beta}_0}(x)\right) = \frac{(-x)^{n(n-1)/2}}{\Gamma_n(n)} \sum_{\{\underline{\alpha}\}} \left(\prod_{i=1}^{n} \frac{1}{\omega_i^{\alpha_i}}\right) \det\left(\tilde{\boldsymbol{\Psi}}_{\underline{\beta}_0,\underline{\alpha}}(x)\right) \quad (39)$$

---

say $\mathbf{x}$ majorizes $\mathbf{y}$ with notation $\mathbf{x} \succ \mathbf{y}$ if $\sum_{k=1}^{p} x_k \geq \sum_{k=1}^{p} y_k, \forall p = 1, ..., q-1$, and $\sum_{k=1}^{q} x_k = \sum_{k=1}^{q} y_k$. A real valued function Θ defined on $A \subset \Re^q$ is said to be Schur-convex on A if $\mathbf{x} \succ \mathbf{y}$ implies $\Theta(\mathbf{x}) \geq \Theta(\mathbf{y})$ [24]. To prove that Θ is Schur-convex, it is sufficient to establish the following two conditions: it is a symmetric function of $\mathbf{x}$, and

$$(x_1 - x_2)\left(\frac{\delta\Theta}{\delta x_1} - \frac{\delta\Theta}{\delta x_2}\right) \geq 0 \quad (50)$$

for all x_1, x_2 [24].

Now consider the specific case when Θ is given by the capacity approximation in (10), ie.

$$\begin{aligned}\Theta &= \log_2\left(1 + \bar{\gamma} g(K)\right) \\ &= \log_2\left(1 + \bar{\gamma} F^{-1}{}_{\lambda_{\max}}\left(\frac{1}{1 + e^{-\sum_{i=1}^{K-1}\frac{1}{i}}}; \omega_1, \omega_2\right)\right)\end{aligned} \quad (51)$$

and let $x_1 = \omega_2$ and $x_2 = \omega_1$ in the $2 \times m$ semi-correlated case we are considering[6]. We can now see that in order to prove the capacity approximation is an increasing function of correlation, it is sufficient to show that it is Schur-convex with respect to (w.r.t.) ω_1 and ω_2. To this end, we must first establish that (51) is symmetric in ω_1 and ω_2. This is immediately verified upon noting that for the $2 \times m$ semi-correlated case [5] (see (52)) where $P(\cdot, \cdot)$ is defined in (30), which is clearly symmetric in ω_1 and ω_2. We must also establish that the second Schur-convexity condition given in (50) is satisfied, ie.

$$\frac{\delta \log_2\left(1 + \bar{\gamma} F^{-1}{}_{\lambda_{\max}}\left(\frac{1}{1+e^{-\sum_{i=1}^{K-1}\frac{1}{i}}}; \omega_1, \omega_2\right)\right)}{\delta\omega_2} - \frac{\delta \log_2\left(1 + \bar{\gamma} F^{-1}{}_{\lambda_{\max}}\left(\frac{1}{1+e^{-\sum_{i=1}^{K-1}\frac{1}{i}}}; \omega_1, \omega_2\right)\right)}{\delta\omega_1} \geq 0 \quad (53)$$

which is the main challenge. After some algebraic manipulation and application of the Implicit Function Theorem, (53) evaluates to

$$\frac{\delta F_{\lambda_{\max}}(g(K); \omega_1, \omega_2)}{\delta\omega_1} - \frac{\delta F_{\lambda_{\max}}(g(K); \omega_1, \omega_2)}{\delta\omega_2} \geq 0 \,. \quad (54)$$

Using (52), (30), and the expansion $e^x = \sum_{k=0}^{\infty} \frac{x^k}{k!}$, we evaluate the condition (54) as follows

$$\begin{aligned}\sum_{k=m}^{\infty} \frac{g^k(K)}{k!(\omega_1\omega_2)^{k-m}} \Bigg(&\frac{\omega_1^{k-m+2} + \omega_2^2\omega_1^{k-m} - \omega_2^{k-m}\omega_1^2}{\omega_2 - \omega_1} \\ &- \omega_2^{k-m+2} + (\omega_1^{k-m} + \omega_2^{k-m}) g(K) \\ &- m(\omega_1^{k-m}\omega_2 + \omega_2^{k-m}\omega_1)\Bigg) + \frac{2g^m(K)}{(m-1)!} \quad \geq \quad 0 \,.\end{aligned} \quad (55)$$

[6]Note that in this section we explicitly show the dependence on ω_1 and ω_2 in the argument of the c.d.f. $F_{\lambda_{\max}}(\cdot)$.

Let us now define the following finite summation

$$\begin{aligned}\Upsilon(c) \triangleq \sum_{k=m}^{m+c} \frac{g^k(K)}{k!(\omega_1\omega_2)^{k-m}} \Bigg(&(\omega_1^{k-m} + \omega_2^{k-m}) g(K) \\ &+ \frac{\omega_1^{k-m+2} + \omega_2^2\omega_1^{k-m} - \omega_2^{k-m}\omega_1^2 - \omega_2^{k-m+2}}{\omega_2 - \omega_1} \\ &\times -m(\omega_1^{k-m}\omega_2 + \omega_2^{k-m}\omega_1)\Bigg) + \frac{2g^m(K)}{(m-1)!} \,.\end{aligned} \quad (56)$$

Note that this is the left-hand side of (55) for $c \to \infty$. After factoring out common terms, we can express (56) according to the following difference equation

$$\begin{aligned}\Upsilon(c) &= \Upsilon(c-1) \\ &+ \frac{g^{m+c}(K)}{(m+c)!(\omega_1\omega_2)^c} \Bigg(\frac{\omega_1^{c+2} + \omega_2^2\omega_1^c - \omega_2^c - \omega_2^{c+2}}{\omega_2 - \omega_1} \\ &\quad + (\omega_1^c + \omega_2^c) g(K) - m(\omega_1^c\omega_2 + \omega_2^c\omega_1)\Bigg)\end{aligned} \quad (57)$$

with

$$\Upsilon(0) = \frac{2g^{m+1}(K)}{m!} \,. \quad (58)$$

Now we establish a sufficient condition such that (55) holds, via induction on $\Upsilon(c)$, using (57). First note that $\Upsilon(0) \geq 0$, since $g(K) > 0$ by definition. We start the induction by assuming that

$$\Upsilon(c-1) \geq 0 \quad (59)$$

and we seek conditions such that $\Upsilon(c) \geq 0$. From (57), this holds if

$$\begin{aligned}\frac{g^{m+c}(K)}{(m+c)!(\omega_1\omega_2)^c} \Bigg(&\frac{\omega_1^{c+2} + \omega_2^2\omega_1^c - \omega_2^c - \omega_2^{c+2}}{\omega_2 - \omega_1} \\ &+ (\omega_1^c + \omega_2^c) g(K) - m(\omega_1^c\omega_2 + \omega_2^c\omega_1)\Bigg) \geq 0 \,.\end{aligned} \quad (60)$$

After some algebraic manipulations, this condition can be rewritten as

$$\begin{aligned}g(K) \geq \frac{\left((\omega_1^2 + \omega_2^2 + m\omega_1(\omega_2 - \omega_1)\right)}{(\omega_2 - \omega_1)\left(\left(\frac{\omega_1}{\omega_2}\right)^c + 1\right)} \\ - \left(\frac{\omega_1}{\omega_2}\right)^c (\omega_1^2 + \omega_2^2 - m\omega_2(\omega_2 - \omega_1))\Bigg)\end{aligned} \quad (61)$$

Since the right hand side (RHS) is a bounded monotonically increasing function of c, the condition in (61) is certainly met if we replace the RHS with its limit as $c \to \infty$, giving the weaker condition as follows

$$g(K) \geq m\omega_1 + \frac{\omega_1^2 + \omega_2^2}{\omega_2 - \omega_1} \,. \quad (62)$$

$$F_{\lambda_{\max}}(x;\omega_1,\omega_2) = \frac{\omega_1\omega_2}{\omega_2-\omega_1}\left(\frac{1}{\omega_1}P\left(m,\frac{x}{\omega_2}\right)P\left(m-1,\frac{x}{\omega_1}\right)\right.$$
$$\left.\times -\frac{1}{\omega_2}P\left(m,\frac{x}{\omega_1}\right)P\left(m-1,\frac{x}{\omega_2}\right)\right) \quad (52)$$

Thus, we have proven that when (62) is satisfied, $\Upsilon(c) \geq 0, \forall c$, thereby establishing that the inequality (55) holds, and hence (54) holds.

Finally, we arrive at the expression in the lemma, by substituting the definition of $g(K)$ given in (11), into (62). □

C. Proof of Theorem 4

We first give the following lemma:

Lemma 2: For sufficiently large K,

$$C_{\text{multi}} = \log_2\left[1+\bar{\gamma}F^{-1}_{\lambda_{\max}}\left(\frac{K}{K+1}\right)\right]. \quad (63)$$

Proof: The proof follows by applying a general result from order statistics [14, Eq. 4.5.1] to C_{multi} in (6), and performing some simple algebraic manipulation. ■

For large K, we need only consider the c.d.f. expansions given in (15), (17) and (18), which are of the form $F(x) = 1-\alpha e^{-ax}x^t$. In addition, these c.d.f. expansions approach the actual c.d.f. for large x. Now the $F^{-1}_{\lambda_{\max}}\left(\frac{K}{K+1}\right)$ term in (63) can be solved by substituting $N(K) = \frac{K}{K+1}$ and $J(x) = x^t$ into the iteration (19) given in Section IV. As K is large, only one iteration is needed, since more iterations would produce nested $\ln$ terms which have negligible effect. This gives for large K

$$\begin{aligned} C_{\text{multi}} &= \log_2\left(1+\frac{\bar{\gamma}}{a}[\ln K + \ln\alpha + \mathcal{O}(\ln\ln K)]\right) \quad (64)\\ &= \log_2 \ln K + \log_2\left(\frac{\bar{\gamma}}{a}\right) + \log_2\left(\frac{a}{\bar{\gamma}\ln K}+1\right.\\ &\qquad \left.+\frac{\ln\alpha}{\ln K}+\mathcal{O}\left(\frac{\ln\ln K}{\ln K}\right)\right)\\ &= \log_2 \ln K + \log_2\left(\frac{\bar{\gamma}}{a}\right) + \log_2\left(1+\mathcal{O}\left(\frac{\ln\ln K}{\ln K}\right)\right). \end{aligned}$$

The capacity offset is given by $\text{CO}_\infty = \frac{1}{a}$. The proof follows by substituting the specific values of a for the uncorrelated, semi- and double-correlated scenarios, given in (20), (21) and (23) respectively.

References

[1] N. Jindal and A. Goldsmith, "Dirty-paper coding versus TDMA for MIMO broadcast channels," *IEEE Trans. Inform. Theory*, vol. 51, no. 5, pp. 1783–1794, May 2005.

[2] H. Boche and E. A. Jorswieck, "Multiple antenna multiple user channels: Optimisation in low SNR," in *Proc. IEEE Wireless Communications and Networking Conference (WCNC)*, vol. 1, Atlanta, GA, Mar. 2004, pp. 513–518.

[3] P. A. Dighe, R. K. Mallik, and S. S. Jamuar, "Analysis of transmit-receive diversity in Rayleigh fading," *IEEE Trans. Commun.*, vol. 51, no. 4, pp. 694–703, Apr. 2003.

[4] M. Kang and M.-S. Alouini, "A comparative study on the performance of MIMO MRC with and without cochannel interference," *IEEE Trans. Commun.*, vol. 52, no. 8, pp. 1417–1425, Aug. 2004.

[5] ——, "Impact of correlation on the capacity of MIMO channels," in *IEEE Int. Conf. on Commun. (ICC)*, Paris, France, June 2003, pp. 2623–2627.

[6] M. R. McKay, A. J. Grant, and I. B. Collings, "Performance analysis of MIMO-MRC in double-correlated Rayleigh environments," *IEEE Trans. Commun.*, vol. 55, no. 3, pp. 497–507, Mar. 2007.

[7] M. R. McKay and I. B. Collings, "General capacity bounds for spatially correlated Rician MIMO channels," *IEEE Trans. Inform. Theory*, vol. 51, no. 9, pp. 3121–3145, Sept. 2005.

[8] D. Shiu, G. J. Foschini, M. J. Gans, and J. M. Kahn, "Fading correlation and its effect on the capacity of multielement antenna systems," *IEEE Trans. Commun.*, vol. 48, no. 3, pp. 502–513, Mar. 2000.

[9] H. Shin, M. Z. Win, J. H. Lee, and M. Chiani, "On the capacity of doubly correlated MIMO channels," *IEEE Trans. Wireless Commun.*, vol. 5, no. 8, pp. 2253–2265, Aug. 2006.

[10] M. Chiani, M. Z. Win, and A. Zanella, "On the capacity of spatially correlated MIMO Rayleigh fading channels," *IEEE Trans. Inform. Theory*, vol. 49, no. 10, pp. 2363–2371, Oct. 2003.

[11] Q. Zhou and H. Dai, "Asymptotic analysis on spatial diversity versus multiuser diversity in wireless networks," in *Proc. IEEE Int. Conf. on Commun. (ICC)*, Istanbul, Turkey, June 2006, pp. 1464–1469.

[12] D. Park and S. Y. Park, "Effect of transmit antenna correlation on multiuser diversity," in *Proc. IEEE Int. Symp. Inform. Theory (ISIT)*, Adelaide, Australia, Sept. 2005, pp. 1421–1425.

[13] P. Viswanath, D. N. C. Tse, and R. Laroia, "Opportunistic beamforming using dumb antennas," *IEEE Trans. Inform. Theory*, vol. 48, no. 6, pp. 1277–1294, June 2002.

[14] H. David and H. Nagaraja, *Order Statistics*, 3rd ed. John Wiley & Sons, 2003.

[15] M. R. McKay, I. B. Collings, and P. J. Smith, "Capacity and SER analysis of MIMO beamforming with MRC," in *Proc. IEEE Int. Conf. on Commun. (ICC)*, Istanbul, Turkey, June 2006, pp. 1326–1330.

[16] W. V. Zwet, *Convex Transformations of Random Variables*. Mathematical Centre, 1970.

[17] C. Martin and B. Ottersten, "Asymptotic eigenvalue distributions and capacity for MIMO channels under correlated fading," *IEEE Trans. Wireless Commun.*, vol. 3, no. 4, pp. 1350–1359, July 2004.

[18] A. Zanella, M. Chiani, and M. Z. Win, "Performance of MIMO MRC in correlated Rayleigh fading environments," in *Proc. IEEE Veh. Tech. Conf. (VTC)*, Stockholm, Sweden, June 2005, pp. 1633–1637.

[19] R. H. Y. Louie, M. R. McKay, I. B. Collings, and B. Vucetic, "Capacity approximations for multiuser MIMO-MRC with antenna correlation," in *Proc. IEEE Int. Conf. on Commun. (ICC)*, Glasgow, UK, June 2007, pp. 5195–5200.

[20] H. Bölcskei, M. Borgmann, and A. J. Paulraj, "Impact of the propagation environment on the performance of space-frequency coded MIMO-OFDM," *IEEE J. Select. Areas Commun.*, vol. 21, no. 3, pp. 427–439, Apr. 2003.

[21] A. Lozano, A. M. Tulino, and S. Verdu, "High-SNR power offset in multiantenna communication," *IEEE Trans. Inform. Theory*, vol. 51, no. 12, pp. 4134–4151, Dec. 2005.

[22] M. Z. Win, "Distribution-invariant monotonicity theorems on multi-channel diversity," to appear in *IEEE Trans. Wireless Commun.*, 2008.

[23] H. Shin and M. Z. Win, "MIMO diversity in the presence of double scattering," to appear in *IEEE Trans. Inform. Theory*, 2008. [Online]. Available: http://arxiv.org/abs/cs.IT/0511028

[24] A. W. Marshall and I. Olkin, *Inequalities: Theory of Majorization and Its Applications*, 1st ed. New York: Academic Press, 1979.

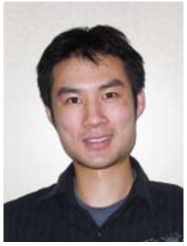

Raymond H. Y. Louie (S'06) received the combined B.E. degree in Electrical Engineering and B.Sc. degree in computer science from the University of New South Wales, Sydney, Australia, in 2006. He is currently working toward the Ph.D. degree in Electrical Engineering at The University of Sydney, Sydney, Australia. His current research interests include ad hoc networks, MIMO systems, and multivariate statistical theory.

His research is supported by a postgraduate scholarship from the Information and Communication Technologies (ICT) Centre at Australia's Commonwealth Scientific and Industrial Research Organization (CSIRO) and an Australian Postgraduate Award (APA).

Matthew R. McKay (S'03) received the combined B.E. degree in Electrical Engineering and B.IT. degree in Computer Science from the Queensland University of Technology, Australia, in 2002, and the Ph.D. degree in Electrical Engineering from the University of Sydney, Australia, in 2006. He then worked as a Research Scientist at the Commonwealth Science and Industrial Research Organization (CSIRO), Sydney, Australia, prior to joining the faculty at the Hong Kong University of Science and Technology (HKUST) in 2007, where he is currently an Assistant Professor. He is also a member of the Center for Wireless Information Technology at HKUST.

His research interests include communications and signal processing; in particular the analysis and design of MIMO systems, random matrix theory, information theory, and wireless ad-hoc and sensor networks.

He was awarded a 2006 Best Student Paper Award at IEEE ICASSP'06, and was jointly awarded the 2006 Best Student Paper Award at IEEE VTC'06-Spring. He was also awarded the University Medal upon graduating from the Queensland University of Technology.

Iain B. Collings (S'92-M'95-SM'02) received the B.E. degree in Electrical and Electronic Engineering from the University of Melbourne in 1992, and the Ph.D. degree in Systems Engineering from the Australian National University in 1995.

Currently he is a CEO Science Leader at the Australian CSIRO, working in the Wireless Technologies Laboratory, ICT Centre. Prior to this he was an Associate Professor at the University of Sydney (1999-2005); a Lecturer at the University of Melbourne (1996-1999); and a Research Fellow in the Australian Cooperative Research Centre for Sensor Signal and Information Processing (1995). He has published over 130 research papers in the area of mobile digital communications. More specifically, channel estimation and adaptive multi-carrier modulation, for time-varying, multi-user, and MIMO channels.

Dr. Collings currently serves as an Editor for the *IEEE Transactions on Wireless Communications*, and for the *Elsevier Physical Communication Journal* (PHYCOM). He has served as the Vice Chair of the Technical Program Committee for IEEE Vehicular Technology Conf. (Spring) 2006, as well as serving on a number of other TPCs and organizing committees of IEEE conferences. He is a founding organizer of the Australian Communication Theory Workshops $2000-08$. He is also the Chair of the IEEE NSW Section Joint Communications and Signal Processing Chapter.